NRC Research Press

ARTICLE

An algebraic input–output equation for planar RRRP and PRRP linkages[1]

Mirja Rotzoll, M. John D. Hayes, and Manfred L. Husty

Abstract: In this paper, the algebraic input–output (IO) equations for planar RRRP and PRRP linkages are derived by mapping the linkage displacement constraints into Study's soma coordinates and then using tangent half-angle substitutions to transform the trigonometric into algebraic expressions. Both equations are found to be equivalent to the one that has already been derived for RRRR linkages, giving exciting new insight into kinematic analysis and synthesis of planar four-bar linkages. The algebraic properties of the IO curve equations yield information regarding the topology of the linkage, such as the sliding position limits of the prismatic joints and (or) the angle limits of the rotational joints. Additionally, the utility of the equations is successfully demonstrated with two approximate synthesis examples.

Key words: function generator, four-bar linkages, Study soma coordinates.

Résumé : Dans cet article, les équations algébriques d'entrée–sortie (IO) pour les liaisons planaires RRRP et PRRP sont dérivées en cartographiant les contraintes de déplacement de la liaison dans les coordonnées soma de Study, puis en utilisant des substitutions tangent-demi angle pour transformer la métrique trigono en expressions algébriques. Les deux équations se sont avérées équivalentes à celle qui a déjà été dérivée pour les liaisons RRRR, donnant un nouvel aperçu passionnant de l'analyse cinématique et de la synthèse des liaisons planaires à quatre barres. Les propriétés algébriques des équations de la courbe IO fournissent des informations sur la topologie de la liaison, telles que les limites de position de glissement des joints prismatiques et (ou) les limites d'angle des joints de rotation. En outre, l'utilité des équations est démontrée avec succès par deux exemples de synthèse approximative. [Traduit par la Rédaction]

Mots-clés : générateur de fonctions, liens à quatre barres, coordonnées soma de Study.

1. Introduction

Freudenstein (1954) developed an elegant trigonometric equation for planar four-bar linkages connected by four rotational (R) joints. The equation, nowadays known as the Freudenstein equation, is widely used in function-generator analysis and synthesis theory. It gives designers a tool to identify the link lengths of mechanisms that optimally transform, typically in a least-squares sense, a specific input angle into a desired output angle governed by a specified functional relation, $f(\psi) = \phi$. Let d be the distance between the centres of the R joints connected to the relatively nonmoving base; a the driver or input link length, which is moving with an angle ψ; b the follower or output link length, which is moving with an angle ϕ; and c the coupler length of a planar RRRR linkage, see Fig. 1. Then, the displacement of the mechanism in terms of the link lengths a, b, c, d, the input angle ψ, and the output angle ϕ is governed by the following input–output (IO) equation:

$$k_1 + k_2 \cos(\phi_i) - k_3 \cos(\psi_i) = \cos(\psi_i - \phi_i) \quad (1)$$

Received 12 July 2019. Accepted 22 January 2020.

M. Rotzoll and M.J.D. Hayes.* Department of Mechanical and Aerospace Engineering, Carleton University, Ottawa, ON K1S 5B6, Canada.

M.L. Husty. Unit Geometry and CAD, University of Innsbruck, 6020 Innsbruck, Austria.

Corresponding author: M. John D. Hayes (email: john.hayes@carleton.ca).

*M. John D. Hayes currently serves as a Guest Editor; peer review and editorial decisions regarding this manuscript were handled by Scott Nokleby.

[1]This paper is part of a Special Issue with the best papers presented during the 2019 CCToMM Symposium on Mechanisms, Machines, and Mechatronics.

Fig. 1. Planar 4R function generator.

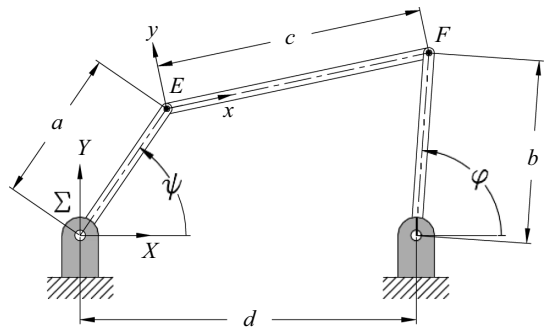

Equation 1 is linear in the k_i Freudenstein parameters, which are defined in terms of the link length ratios as

$$k_1 = \frac{\left(a^2 + b^2 + d^2 - c^2\right)}{2ab} \qquad k_2 = \frac{d}{a} \qquad k_3 = \frac{d}{b}$$

In Hayes et al. (2018), they provide an alternative derivation of a general algebraic IO equation for the same type of mechanism:

$$(2) \qquad Au^2v^2 + Bu^2 + Cv^2 - 8abuv + D = 0$$

where

$$A = (a - b - c + d)(a - b + c + d) = A_1A_2$$
$$B = (a + b - c + d)(a + b + c + d) = B_1B_2$$
$$C = (a + b - c - d)(a + b + c - d) = C_1C_2$$
$$D = (a - b + c - d)(a - b - c - d) = D_1D_2$$
$$u = \tan\frac{\psi}{2}$$
$$v = \tan\frac{\phi}{2}$$

Equation 2 is an algebraic quartic equation in terms of input and output joint angle parameters u and v. It was obtained by mapping the linkage constraint equations of the input and output links, i.e., circular motion for the distal R joints, into Study's soma coordinates (Study 1903; Bottema and Roth 1990), converting the trigonometric expressions into algebraic ones by applying the tangent of the half-angle, or Weierstraß substitutions (Bradley and Smith 1995), and finally eliminating the Study coordinates to obtain the quartic IO curve (Hayes et al. 2018; Husty and Pfurner 2018). The soma coordinates are used to represent distinct spatial rigid body displacements in three-dimensional Euclidean space as distinct points in a higher dimensional projective space. Eight projective soma coordinates result from mapping a displacement to the seven-dimensional projective kinematic mapping image space. A displacement can be represented in Euclidean space as a change in position and orientation of a moving coordinate system expressed with respect to a nonmoving one. The first four soma coordinates are typically established as the four Euler rotation parameters (Bottema and Roth 1990; Husty et al. 1997) to quantify the new orientation, while the remaining four represent the translation component of the displacement and are obtained as distinct linear combinations of the Cartesian coordinates of the new location of the origin of the moving coordinate system and the Euler parameters. For planar displacements, two of the Euler parameters and two of the translation parameters are identically zero.

We believe that this new method for determining the IO equation can be further expanded to four-bar mechanisms of any topology for planar, spherical, and spatial mechanisms. Ultimately, this would provide designers with a versatile tool for optimal synthesis of function-generating mechanisms. While others have examined the possibilities of a unified approach to four-bar mechanism analysis and synthesis, see Bai and Angeles (2008) for example, proposed methods failed to identify a single algebraic and constraint-based IO equation that is truly generalised to four-bars containing two, one, or no prismatic (P) joints. Planar four-bar mechanisms containing more than two P joints result in linear IO relations and can only generate translations. Hence, they are not considered herein.

In this paper, we will derive the algebraic IO equations for RRRP and PRRP linkages using the same technique developed in Hayes et al. (2018). The main goal is to demonstrate that the method of deriving the algebraic forms of the IO equations using Study's soma and elimination theory (Salmon 1885; Cox et al. 1997) lead to precisely the same equation, namely eq. 2, with only the roles of constant and variable changing for certain design parameters. We will then interpret some important characteristics of the resulting algebraic IO curves in the coordinate plane of the input and output variables employing the theory of planar algebraic curves (Harnack 1876; Salmon 1879*a*, 1879*b*; Hilton 1920; Primrose 1955; Husty et al. 1997). Finally, we will illustrate these characteristics with two function-generator approximate synthesis examples using the algebraic form of the associated IO equation.

2. Algebraic IO equation for RRRP function generators

The planar RRRP linkage, also called a crank-slider, is a widely used mechanism found in a variety of applications, such as piston-cylinder engines or reciprocating pumps (Wunderlich 1970; Uicker et al. 2017). This linkage transforms a rotational input motion into a reciprocating translational output motion. A schematic of the linkage type is shown in Fig. 2. In the first step, as in the derivation of eq. 2, the displacement constraints of the driver and follower have to be defined (Hayes et al. 2018; Husty and Pfurner 2018). For that purpose, let Σ_1 be a fixed Cartesian coordinate system whose origin is at the centre of the ground-fixed driver R joint, E the

Fig. 2. Planar RRRP function generator.

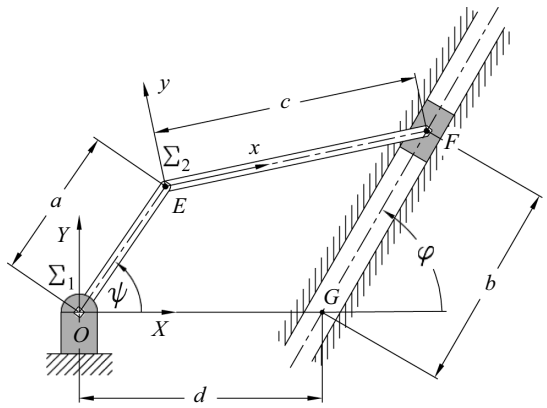

intersection point of the driver and coupler link centre lines, and F the intersection point of the coupler and the follower link centre lines. While point E is moving on a circle with a radius of length a around the origin O of Σ_1, F is moving on a line that intersects the baseline at point G making a fixed angle ϕ at a distance d from the origin of Σ_1. Hence, the positions of E and F can be described as points in Σ_1 by the following array element constraint equations:

$$(3)\qquad \begin{aligned} X_E - a\,\cos\psi &= 0 \\ Y_E - a\,\sin\psi &= 0 \end{aligned}$$

$$(4)\qquad \begin{aligned} X_F - d - b\,\cos\phi &= 0 \\ Y_F - b\,\sin\phi &= 0 \end{aligned}$$

$$(7)\qquad \left.\begin{aligned} -a\,\cos\psi(x_0^2+x_3^2) + 2(-x_0y_1+x_3y_2) &= 0 \\ -a\,\sin\psi(x_0^2+x_3^2) - 2(x_0y_1+x_3y_2) &= 0 \\ -(b\,\cos\varphi+d)(x_0^2+x_3^2) + c(x_0^2-x_3^2) + 2(-x_0y_1+x_3y_2) &= 0 \\ -b\,\sin\varphi(x_0^2+x_3^2) + 2c(x_0x_3) - 2(x_0y_1+x_3y_2) &= 0 \end{aligned}\right\}$$

The tangent of the half angle substitutions

$$(8)\qquad u = \tan\frac{\psi}{2} \qquad v = \tan\frac{\phi}{2}$$

$$(9)\qquad \cos\psi = \frac{1-u^2}{1+u^2} \qquad \sin\psi = \frac{2u}{1+u^2}$$

$$(10)\qquad \cos\phi = \frac{1-v^2}{1+v^2} \qquad \sin\phi = \frac{2v}{1+v^2}$$

are used to transform the trigonometric constraint-based relations in eq. 7 to algebraic equations. After eliminating the image space coordinates x_i and y_i using resultants and elimination theory, then collecting the results for the variables u and b, the following algebraic IO equation emerges:

Note that these constraint equations are identical to those formulated for the 4R linkage in Hayes et al. (2018), but where the roles of b and ϕ are reversed: b here is a variable distance and ϕ is a fixed angle. This allows us to proceed in determining the IO equation in the same manner. Let Σ_2 be a coordinate frame, which moves with the coupler, whose origin is centred at E with x-axis pointing towards F. Then the homogeneous transformation matrix, expressed in soma coordinates ($x_0 : x_3 : y_1 : y_2$), between the two coordinate frames is given by Hayes et al. (2018)

$$(5)\qquad \mathbf{T} = \frac{1}{x_0^2+x_3^2}\begin{bmatrix} x_0^2+x_3^2 & 0 & 0 \\ 2(-x_0y_1+x_3y_2) & x_0^2-x_3^2 & -2x_0x_3 \\ -2(x_0y_2+x_3y_1) & 2x_0x_3 & x_0^2-x_3^2 \end{bmatrix}$$

For example, a point (x, y) in Σ_2 can be expressed as a point (X,Y) in Σ_1 using the coordinate transformation

$$(6)\qquad \begin{bmatrix} 1 \\ X \\ Y \end{bmatrix} = \mathbf{T}\begin{bmatrix} 1 \\ x \\ y \end{bmatrix}$$

Now, in the coordinate frame Σ_2, the two end points of the coupler E and F have coordinates $(x,y) = (0,0)$ and $(c,0)$, respectively. These are transformed using eq. 6 to their representations in Σ_1, and the results are equated to the coordinates for points E and F in eqs. 3 and 4, which, when simplified, reveal the following four array element position constraint equations in terms of the link lengths, input and output angles ψ and ϕ, as well as the four soma coordinates x_0, x_3, y_1, and y_2:

$$(11)\qquad k := Au^2b^2 + Bb^2 + Cu^2b - 8abuv + Db + Eu^2 + F = 0$$

where

$$\begin{aligned} A &= v^2+1 \\ B &= v^2+1 \\ C &= -2(v-1)(v+1)(a+d) \\ D &= 2(v-1)(v+1)(a-d) \\ E &= (v^2+1)(a+c+d)(a-c+d) \\ F &= (v^2+1)(a+c-d)(a-c-d) \end{aligned}$$

By rearranging eq. 11, it can easily be shown that it is identical to eq. 2 when the terms multiplying u and v are collected and factored instead of u and b. The difference from a designers' perspective is only that the variables of the 4R linkage are the IO angle parameters u and v, while those for the RRRP linkage are the input angle parameter u and output slider distance b.

2.1. Interpretation of the RRRP IO equation

Analysing eq. 11 using the theory of planar algebraic curves (Primrose 1955; Husty et al. 1997) one can see that it has the following characteristics, which are independent of the constant design parameter lengths a, c, d, and constant angle parameter v.

1. Equation 11 is of degree $n = 4$ in variables u and b.
2. It contains two double points, DP = 2, each located at the intersections with the line at infinity of the u- and b-axis in the u–b variable design parameter plane.
3. It has genus $p = 1$; hence, it is an elliptic curve and the maximum number of assembly modes of the linkage becomes $m = p + 1 = 2$ (Harnack 1876; Husty and Pfurner 2018).

These three characteristics are now proved to be true for all nondegenerate planar RRRP linkages. The first item is obvious by inspection. The proof of the second item requires that eq. 11 be homogenised. If we use the arbitrary homogenising coordinate w we obtain

$$(12)\quad k_h := Au^2b^2 + Bb^2w^2 + Cu^2bw - 8avubw^2 + Dbw^3 + Eu^2w^2 + Fw^4 = 0$$

which now contains seven terms all homogeneously of degree $n = 4$ in terms of u, b, and w. The three partial derivatives of k_h with respect to the three variable coordinates u, b, and w are all homogeneously of degree $n = 3$:

$$(13)\quad \left.\begin{aligned} \frac{\partial k_h}{\partial u} &= 2Aub^2 + 2Cubw - 8avbw^2 + 2Euw^2 = 0 \\ \frac{\partial k_h}{\partial b} &= 2Au^2b + 2Bbw^2 + Cu^2w - 8avuw^2 + Dw^3 = 0 \\ \frac{\partial k_h}{\partial w} &= 2Bb^2w + Cu^2b - 16avubw + 3Dbw^2 + 2Eu^2w + 4Fw^3 = 0 \end{aligned}\right\}$$

Equations 12 and 13 have two common solutions that are independent of the link lengths a, c, and d, as well as angle parameter v, which are embedded in the coefficients A, B, C, D, E, and F:

$$(14)\quad S_1 := \{u = 1, b = 0, w = 0\} \qquad S_2 := \{u = 0, b = 1, w = 0\}$$

These two points, called double points, common to all algebraic IO curves for every planar RRRP four-bar mechanism are the points on the line at infinity $w = 0$ of the u- and b-axes, respectively. Each of these double points can have real or complex tangents depending on the values of the three constant link lengths a, c, and d, which in turn determines the nature of the mobility of the linkage. As these two double points are uniquely defined relative to the regular points on the curve, they are also known as singular points (Hilton 1920; Primrose 1955).

The discriminant of eq. 12, evaluated at a double point, reveals whether that double point has a pair of real or complex conjugate tangents (Hilton 1920; Husty et al. 1997) in turn yielding information about the topology of the mechanism (Hilton 1920; Husty and Pfurner 2018). If the tangents are complex conjugates, the double point is an acnode: a hermit point that satisfies the equation of the curve but is isolated from all other points on the curve. If this is the case then the slider travel, represented by b, is restricted. The discriminant and the meaning of its value are (Hilton 1920; Husty et al. 1997)

$$\Delta = \left(\frac{\partial^2 k_h}{\partial u\,\partial w}\right)^2 - \frac{\partial^2 k_h}{\partial u^2}\frac{\partial^2 k_h}{\partial w^2} \begin{cases} >0 \Rightarrow \text{two real distinct tangents(crunode)} \\ =0 \Rightarrow \text{tworeal coincident tangents(cusp)} \\ <0 \Rightarrow \text{two complex conjugate tangents(acnode)} \end{cases}$$

For the homogeneous IO equation of an RRRP linkage, eq. 12, the discriminant of the point at infinity $(u : b : w) = (0 : 1 : 0)$ on the b-axis is

$$(15)\quad \Delta = -4(v^2 + 1)^2$$

meaning that the double point associated with the output slider is always an acnode independently of the link lengths and orientation of the slider. It should not surprise that the discriminant of eq. 12 is always negative, as the slider must always have finite translation limits.

To determine whether the rotational input link is a crank or a rocker, it is sufficient to determine if the numerical value of the coefficient E in eq. 11 is <0 when the coordinates in Σ_1 are transformed by the rotation about O_{Σ_1} required to make $v = 1$, i.e., $\phi = \pi/2$. As the two factors $(v^2 + 1)$ and $(a + c + d)$ in E must always be >0, it is a simple matter to show that the condition for input link a to be a crank reduces to

$$(16)\quad a - c + d < 0$$

The proof for the third item comes from the definition of genus, which in this case is the difference between the maximum number of double points for a curve of degree $n = 4$ and the actual number of double points it

Fig. 3. RRRP where $a = 2.8$, $c = 1.7$, $d = 1$, and $v = 1.5$. [Colour online.]

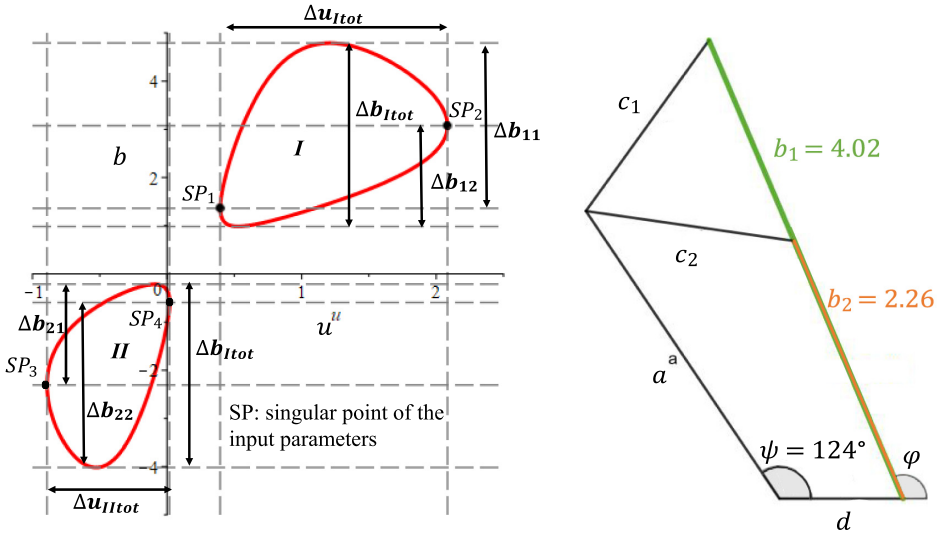

possesses. The maximum number of double points, DP_{max}, for an arbitrary algebraic curve of degree n is given by Hunt (1978)

$$DP_{max} = \frac{1}{2}(n-1)(n-2)$$

The maximum number of double points for a curve of degree $n = 4$ is 3. We see that because the algebraic IO curve has only 2 double points, it is deficient by 1; hence, its genus is $p = 1$. Because of this, it cannot be parameterised, and it is defined to be an elliptic curve (Primrose 1955). This definition does not mean that the curve has the form of an ellipse, rather that the curve can be expressed, with a suitable change of variables, as an elliptic curve. In the plane, every elliptic curve with real coefficients can be put in the standard form

$$x_2^2 = x_1^3 + Ax_1 + B$$

for some real constants A and B. We now consider some illustrative RRRP examples.

2.1.1. Example 1. Design parameter selection: $a = 2.8$; $c = 1.7$; $d = 1$; $v = 1.5$

With the chosen design parameters, the input link a is a rocker because eq. 16 is >0 for some $-\pi \le \psi \le \pi$. Two different assembly modes I and II can be identified examining Fig. 3. Each assembly mode has two locations where the mechanism is positioned at an input singular configuration where the tangents of the IO equation are vertical, separating each assembly mode into two working modes. If the link is assembled according to the upper right part of the curve (assembly mode I), Δu_{Itot} and Δb_{Itot} correspond to the maximum swing angle and maximum sliding position, respectively. Considering each working mode separately, Δb_{11} and Δb_{12} correspond to the maximum sliding position in assembly mode I. Similarly, if the link is assembled according to the lower left part of the curve (assembly mode II), Δu_{IItot} and Δb_{IItot} correspond to the maximum swing angle and maximum sliding position. The maximum sliding positions for each working mode are Δb_{21} and Δb_{22}.

2.1.2. Example 2. Design parameter selection: $a = 2.8$; $c = 1.7$; $d = 1$; $v = 0$

Taking the same design parameters, but changing the orientation of the slider to $v = 0$ reveals a representation of the IO equation as shown in Fig. 4. Again, examining eq. 16 shows that the expression is not <0 for every $-\pi \le \psi \le \pi$, and hence, the input link is a rocker. The linkage is once again split into two assembly modes, I and II. Due to the chosen parametrisation according to eq. 8 and as $\psi = \pi$ is included in assembly mode I, the graph contains the point at $u = \pm\infty$, explaining the asymptotes of the IO equation. The maximum swing angle, as well as the maximum sliding position, can be evaluated analogous to the previous example.

2.1.3. Example 3. Design parameter selection: $a = 2$; $c = 2.5$; $d = 1$; $v = 0.2$

These design parameters yield the IO equation illustrated in Fig. 5. In contrast to the previous examples, eq. 16 is <0 meaning that the input link a can fully rotate. This linkage also possesses two assembly modes, I and II, resulting in identical maximum sliding position, $\Delta b_{Itot} = \Delta b_{IItot}$. In this example, points where the mechanism is located at an input singular configuration do not exist. The output linkage movement is unambiguously defined via the linkage assembly.

2.1.4. Example 4. A very special RRRP linkage arises when $a = c$ and $v = 0$

With these conditions, the factors of eq. 11 simplify to

$$(b+d)(bu^2 + 2cu^2 + du^2 + b - 2c + d) = 0 \quad (17)$$

Fig. 4. RRRP where $a = 2.8$, $c = 1.7$, $d = 1$, and $v = 0$. [Colour online.]

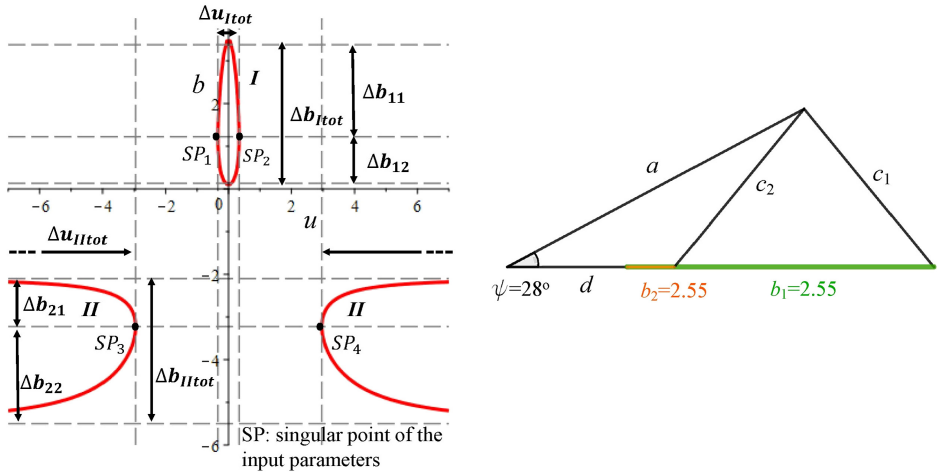

Fig. 5. RRRP where $a = 2$, $c = 2.5$, $d = 1$, and $v = 0.2$. [Colour online.]

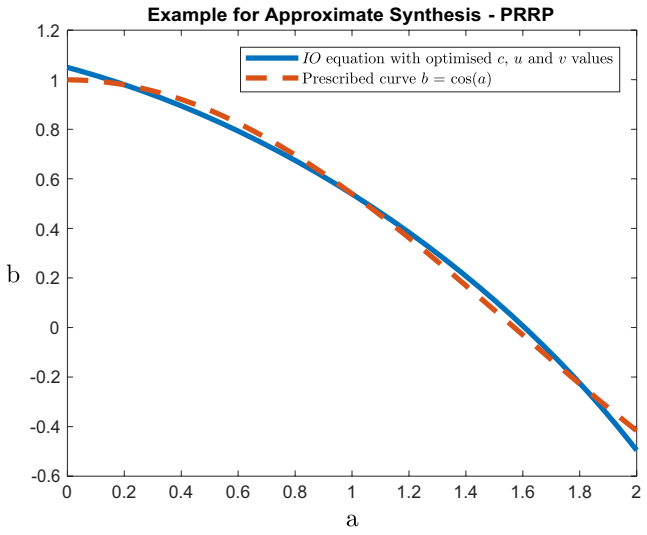

As a result, this special IO equation is decomposed into two operation modes. Moreover, two additional double points can be observed. These double points, the bifurcation points, BP_1 and BP_2, are always located at BP_1 (+1, –d) and BP_2 (–1, –d).

This IO equation has four different working modes, the input link a is able to rotate completely, and the mechanism has the ability to fold. From eq. 17, the global maximum is found at $b_{max} = 2c - d$ and the global minimum is the asymptote at $b_{max} = -2c - d$, which leads to the following four maximum sliding positions of $\Delta b_{i_{max}}$:

$$(18)\quad \Delta b_{1_{max}} = 4a = 4c \qquad \Delta b_{2_{max}} = 2c \qquad \Delta b_{3_{max}} = 2c \qquad \Delta b_{4_{max}} = 0$$

An example of the IO equation (where $a = c = 1.7$ and $d = 1$) is illustrated in Fig. 6.

2.2. RRRP approximate synthesis

To show that eq. 11 can be used to generate arbitrary functions of the form $f(\psi) = b$, an example approximating the curve

$$(19)\quad b = \cos(\psi)$$

is considered. For this example, 50 sample points were evenly distributed within the interval $-3 \le u \le 3$.

The Newton–Gauss algorithm was used to iteratively minimise the structural error, the error residual found between the prescribed curve and the curve generated by the linkage (Tinubu and Gupta 1984). The optimised function approximation with an RRRP linkage is obtained with the identified design parameters $a = 0.9426$, $c = 1.1587$, $d = 1$, and $v = 1.5 \times 10^{-5}$.

Fig. 6. RRRP where $a = c = 1.7$, $d = 1$, and $v = 0$. [Colour online.]

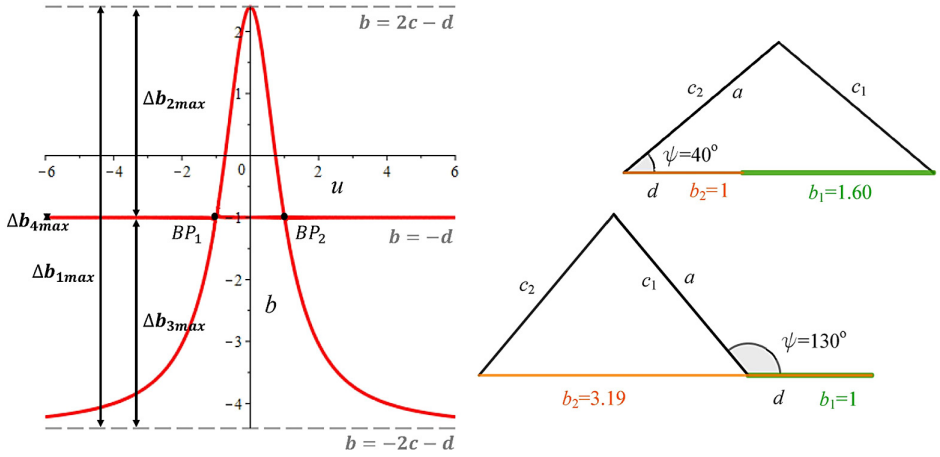

Fig. 7. RRRP where $a = 0.9426$, $c = 1.1587$, $d = 1$, and $v = 1.5 \times 10^{-5}$. [Colour online.]

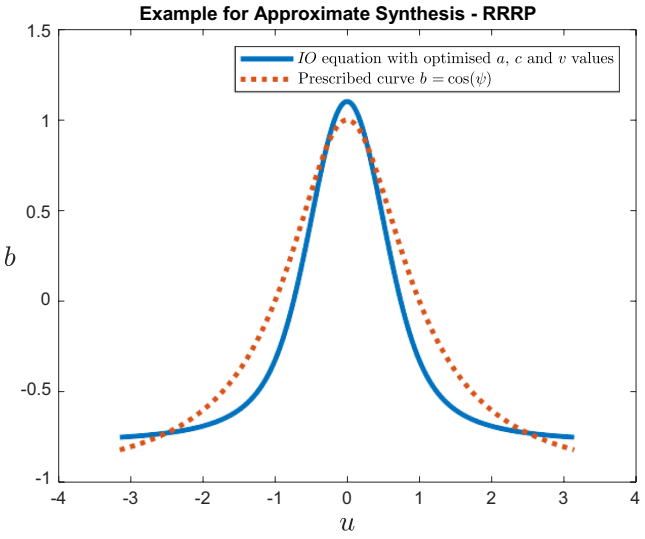

Figure 7 illustrates the structural error of the identified linkage. This example underscores the applicability of the general algebraic IO equation for RRRP in addition to RRRR linkages.

3. Algebraic equation for PRRP function generators

As it was demonstrated that the general algebraic IO equation is useful for RRRP mechanism synthesis, it is reasonable to expect that the equation is equally valid for PRRP mechanisms. We will not consider mechanisms with greater than two P joints as such linkages can only generate translations. The PRRP mechanism consists of one prismatic, two rotational, and another prismatic joint. In addition to a translational output motion b, the input motion a of the function generator is also a translation governed by a functional relation expressed by $f(a) = b$. The most common configuration is the elliptical trammel whose P-joint directions are perpendicular to each other, but for a general PRRP mechanism the P-joint axes may have any nonzero angle between them, as illustrated in Fig. 8.

As the two P joints are both moving on a line, the initial constraint equations for the PRRP can again be set up according to eqs. 3 and 4. Note that in this particular case, the variables of the IO equation become a and b, while u, v, c, and d represent the design parameters. According to the same derivation for the RRRP and the RRRR function generators, but instead treating both a and b as variables, the IO equation of the function generator becomes

$$Aa^2 + Bb^2 + Cab + Da + Eb + F = 0 \quad (20)$$

where the coefficients are factors of constants u, c, d, and v:

$$\begin{aligned} A &= (v^2+1)(u^2+1) \\ B &= (v^2+1)(u^2+1) \\ C &= -2(uv-u+v+1)(uv+u-v+1) \\ D &= 2d(v^2+1)(u-1)(u+1) \\ E &= -2d(v-1)(v+1)(u^2+1) \\ F &= -(v^2+1)(u^2+1)(c-d)(c+d) \end{aligned}$$

Again, by collecting the variables in a different way it can easily be shown that eq. 20 is identical to eqs. 2 and 11.

3.1. Interpretation of the PRRP IO equation

Equation 20 has the following characteristics:

1. It is of degree $n = 2$.
2. It is a quadratic equation in two variables; thus, the IO equation is a conic section.
3. Its IO curve possesses genus $p = 0$; hence, the maximum number of assembly modes of the linkage is $m = p + 1 = 1$ (Harnack 1876; Husty and Pfurner 2018).

Fig. 8. A PRRP linkage.

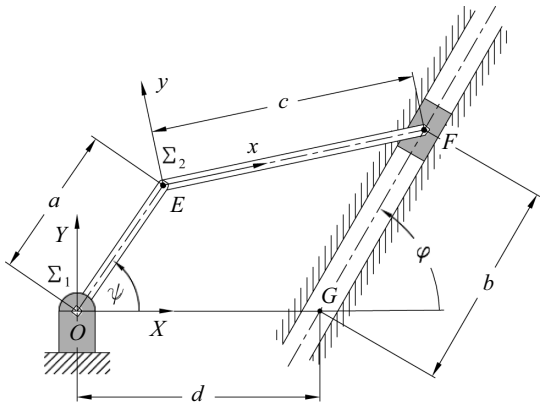

From the discriminant, Δ_q, of the quadratic form associated with the conic section implied by eq. 20

$$\Delta_q = \begin{vmatrix} A & C/2 \\ C/2 & B \end{vmatrix} \tag{21}$$

we can, according to Table 1, determine whether the conic is an ellipse, parabola, or hyperbola (Glaeser et al. 2016). For eq. 20 the discriminant reduces to

$$\begin{vmatrix} (v^2+1)(u^2+1) & -(uv-u+v+1)(uv+u-v+1) \\ -(uv-u+v+1)(uv+u-v+1) & (v^2+1)(u^2+1) \end{vmatrix} = 4(uv+1)^2(u-v)^2 \tag{22}$$

Because eq. 22 is independent of link lengths then $\Delta_q \geq 0$ for all PRRP linkages and the conic represented by eq. 20 can never be an hyperbola. The graph of the IO equation is always an ellipse with but one exception: if $u = -1/v$ or $u = v$, the conic becomes a special parabola, i.e., two parallel lines. A distinguished ellipse, the circle, arises when $A = B$ and $C = 0$, which are the cases for

$$u = \pm 1 \qquad v = 0 \qquad u = 0 \qquad v = \pm 1 \tag{23}$$

i.e., when the axes are perpendicular to each other. These findings align with the literature (Sangwin 2009) proving that this type of mechanism generates an ellipse, confirming the validity of the derived PRRP IO equation.

3.1.1. *Example 5. Design parameter selection: v = 1.7; u = 0.8; c = 2; d = 1*

Figure 9 illustrates the maximum sliding positions a_{tot} and b_{tot}. Considering a to be the input slider, two singular points separate the curve into two working modes. Hence, the output slider can have two different maximum sliding positions Δb_1 and Δb_2.

3.2. PRRP approximation synthesis

To show that eq. 20 can also be used to generate a general function $f(a) = b$, we now consider an example where the desired function is

$$b = \cos(a) \tag{24}$$

For this example, 50 sample points are selected to be evenly distributed within the interval $0 \leq a \leq 2$. Again, the Newton–Gauss algorithm is used to minimise the structural error. As a result, the best approximation with a PRRP linkage is obtained with the identified constants $c = 2.0313$, $d = 1$, $u = -1.1868$, and $v = 0.1353$, or $c = 2.0313$, $u = 1.1868$, and $v = -0.1353$. The designer may choose between these two different assembly modes. The structural error is illustrated in Fig. 10. The desired curve is illustrated in red, and the blue curve represents the approximation obtained by the PRRP linkage. For this example, the approximation obtained by the PRRP function generator is notably close to the prescribed curve. Hence, this example confirms the applicability of eq. 20 for approximate synthesis problems.

Table 1. Impact of the discriminant value on the shape of function the PRRP can generate.

Discriminant of a nondegenerated conic	Shape
$\Delta_q > 0$	Ellipse
$\Delta_q = 0$	Parabola
$\Delta_q < 0$	Hyperbola

4. Conclusions

In this paper, two algebraic IO equations for RRRP and PRRP linkages were derived. It was shown that these equations are identical to the algebraic equation for RRRR linkages derived in Hayes et al. (2018). We believe this to be a remarkable result having never been reported in the vast body of archival literature collected since antiquity! Analysing the equations revealed that the RRRP linkage can have a maximum of two assembly modes, which can be divided into two working modes. A folding mechanism occurs if $a = c$ and $v = 0$. The PRRP linkage has only one assembly mode. It was demonstrated that its IO curve is either an ellipse or, if $u = -1/v$ or $u = v$, two parallel lines. Furthermore, both equations were verified by a synthesis example that approximated the respective design parameters. Being able to expand the algebraic IO equation to two additional linkages, RRRP and PRRP, helps designers to choose the optimal linkage with the optimal design parameters with reduced time and effort. The generalisation of this paper

Fig. 9. PRRP where $v = 1.7$, $u = 0.8$, $c = 2$, and $d = 1$. [Colour online.]

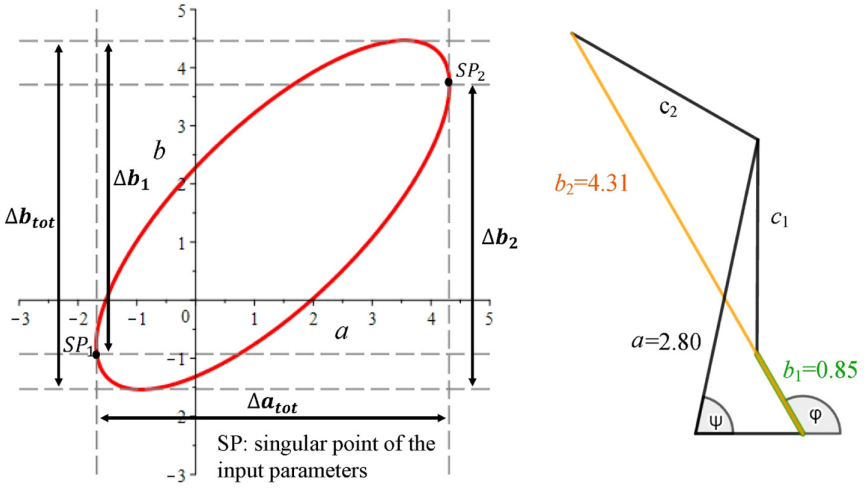

Fig. 10. PRRP where $v = 0.1353$, $u = -1.1868$, $c = 0.3132$, and $d = 1$. [Colour online.]

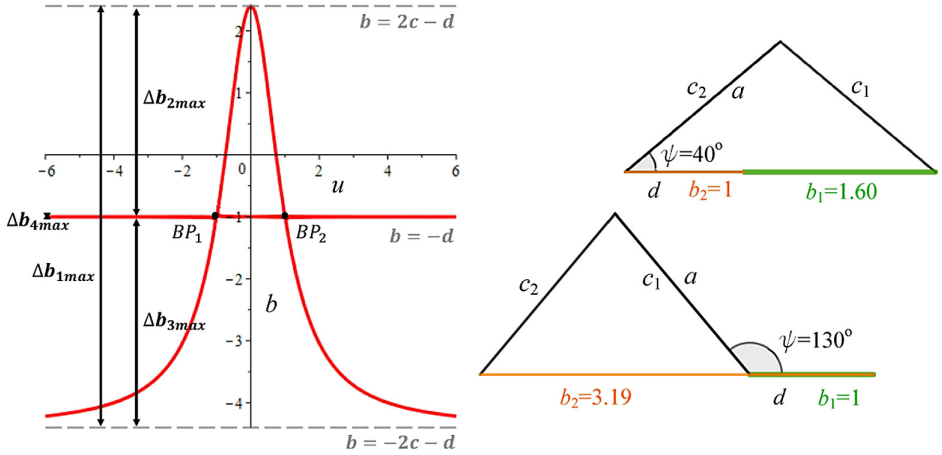

is an important step towards the main goal of synthesising the optimal linkage of planar, spherical, or spatial function generators.

Acknowledgements

The authors are gratefully for the partial financial support of this research by Mitacs Canada through a Globalink Research Grant awarded to the first author.

References

Bai, S., and Angeles, J. 2008. A unified input–output analysis of four-bar linkages. Mech. Mach. Theory, **43**(2): 240–251. doi:10.1016/j.mechmachtheory.2007.01.002.

Bottema, O., and Roth, B. 1990. Theoretical kinematics. Dover Publications, Inc., New York, NY, USA.

Bradley, G.L., and Smith, K.J. 1995. Calculus. Prentice Hall, Englewood Cliffs, NJ, USA.

Cox, D., Little, J., and O'Shea, D. 1997. Ideals, varieties, and algorithms: an introduction to computational algebraic geometry and commutative algebra. 2nd ed. Springer-Verlag, Berlin, Germany.

Freudenstein, F. 1954. Design of four-link mechanisms. Ph.D. thesis, Columbia University, New York, NY, USA.

Glaeser, G., Stachel, H., and Odehnal, B. 2016. The universe of conics: from the ancient greeks to 21st century developments. Springer.

Harnack, A. 1876. Über die Vielteiligkeit der ebenen algebraischen Kurven. Math. Ann. **10**: 189–198.

Hayes, M.J.D., Husty, M.L., and Pfurner, M. 2018. Input-output equation for planar four-bar linkages. International Symposium on Advances in Robot Kinematics. Springer. pp. 12–19.

Hilton, H. 1920. Plane algebraic curves. Clarendon Press, Oxford, UK.

Hunt, K.H. 1978. Kinematic geometry of mechanisms. Clarendon Press, Oxford, UK.

Husty, M., and Pfurner, M. 2018. An algebraic version of the input-output equation of planar four-bar mechanisms. International Conference on Geometry and Graphics, Milan, Italy. pp. 746–757.

Husty, M., Karger, A., Sachs, H., and Steinhilper, W. 1997. Kinematik und Robotik. Springer-Verlag, Berlin, Germany.

Primrose, E.J.F. 1955. Plane algebraic curves. MacMillan.

Salmon, G. 1879*a*. A treatise on conic sections. 6th ed. Longmans, Green, and Co., London, UK.

Salmon, G. 1879*b*. A treatise on the higher plane curves. 3rd ed. Hodges, Foster, and Figgis, Dublin, Ireland.

Salmon, G. 1885. Lessons introductory to the modern higher algebra. 4th ed. Hodges, Foster, and Figgis, Dublin, Ireland.

Sangwin, C. 2009. The wonky trammel of Archimedes. Teach. Math. Appl.: Int. J. IMA, **28**(1): 48–52. doi:10.1093/teamat/hrn019.

Study, E. 1903. Geometrie der Dynamen. Teubner Verlag, Leipzig, Germany.

Tinubu, S.O., and Gupta, K.C. 1984. Optimal synthesis of function generators without the branch defect. J. Mech. Transm. Autom. Des. **106**(3): 348–354. doi:10.1115/1.3267418.

Uicker, J.J., Pennock, G.R., and Shigley, J.E. 2017. Theory of machines and mechanisms. 5th ed. Oxford University Press, New York, NY, USA.

Wunderlich, W. 1970. Ebene kinematik. Hochschultaschenbücher-Verlag, Mannheim, Germany; Wien, Austria; Zürich, Switzerland.